Uplink Interference Mitigation for OFDMA Femtocell Networks

Yanzan Sun, Roger Piqueras Jover, Xiaodong Wang
Electrical Engineering Department
Columbia University
New York, NY 10027

Abstract

Femtocell networks, consisting of a conventional macro cellular deployment and overlaying femtocells, forming a hierarchical cell structure, constitute an attractive solution to improving the macrocell capacity and coverage. However, the inter- and intra-tier interferences in such systems can significantly reduce the capacity and cause an unacceptably high level of outage. This paper treats the uplink interference problem in orthogonal frequency-division multiple-access (OFDMA)-based femtocell networks with partial cochannel deployment. We first propose an inter-tier interference mitigation strategy without the femtocell users power control by forcing the femto-interfering macrocell users to use only some dedicated subcarriers. The non-interfering macrocell users, on the other hand, can use either the dedicated subcarriers, or the shared subcarriers which are also used by the femtocell users. We then propose subcarrier allocation schemes based on the auction algorithm for macrocell users and femtocell users, respectively, to independently mitigate the intra-tier interference. The proposed interference mitigation scheme for femtocell networks offers significant performance improvement over the existing methods by substantially reducing the inter- and intra-tier inferences in the system.

Index Terms

Femtocell, OFDMA, interference mitigation, auction algorithm.

I. Introduction

In recent years, wireless operators have been experiencing a steadily increasing demand for higher data rates and better quality of service due to the constant growth in the number of active wireless terminals. One significant challenge is how to improve the indoor coverage. Studies show that over 50% of all voice calls and more than 70% of data traffic originate from indoors [1]. Therefore, indoor coverage providing high data rate and quality-of-service (QoS) is a key issue in developing next-generation wireless systems. However, adding macrocell base station (MBS) to meet the growing indoor service demands is very expensive. Instead, femtocell access points (FAPs) have been proposed as a new system architecture to tackle this problem [2], [3].

An FAP is a simple, low-power and low-cost base station installed at the user's premise, e.g., house, office, warehouse, etc., that provides local access to the network by means of some cellular technology (e.g., 2G, 3G). Using femtocells benefits both users and operators. Due to the proximity between the transmitter and receiver, indoor users experience better signal quality and communicate with higher throughput. Since most indoor users (e.g., the ones in their own apartments) are connected to an FAP, there are fewer indoor users transmitting in the macrocell and the overall capacity and QoS of the network improves. From the operator's point of view, femtocells can improve spectrum reuse and provide high network capacity and spectral efficiency. In addition, given that FAPs are paid for and maintained by the owners, the operating costs of the network is reduced.

On the other hand, despite these advantages, femtocells bring about multiple new challenges in terms of network architecture, interference management and synchronization [3]. In particular, the interference problem becomes a major issue that requires new solutions due to the extra degrees of complexity in comparison with standard cellular networks.

There are basically three types of deployment configurations for femtocell networks [4]–[6]. The first one is orthogonal deployment, where the spectrum is divided into two independent fragments: one used by the macrocells and the other used by the femtocells [4]. Although this approach can eliminate inter-tier interference, frequency resources are not efficiently utilized. The second is cochannel deployment, in which both macrocells and femtocells have access to all available channels [5]. Such a scheme could generate an excessive levels of interference. The third one is a partial cochannel deployment method, where the whole spectrum is divided into two parts, one dedicated to the macrocells and the other shared by macrocells and femtocells [6]. There are also three types of FAP access methods to allow or restrict its usage by users: open access allowing all users to access; closed access allowing only subscribed users to access, i.e., closed subscriber group (CSG) scheme; hybrid access allowing non-subscribers to use limited amount of femtocell resources.

Previous works in the literature mainly focus on solutions for cochannel assignment and closed access by using power control. Specifically, downlink power control for the FAPs is treated in [7]–[9]; and uplink power control for the femtocell users (FUs) is discussed in [10]–[15]. A distributed channel assignment algorithm for mitigating interference among femtocells is given in [16] without considering the interference from FUs to the MBS. Per-tier outage probability and the transmission capacity in terms of macrocell and femtocell transmission power and cochannel femtocell density are analysed in [17]. The partial cochannel deployment strategy is considered in [18] for the simple scenario of single femtocell within the coverage of MBS. This paper focuses on uplink interference mitigation in the OFDMA femtocell networks that employ the partial cochannel deployment strategy. First, an inter-tier interference mitigation method is proposed according to the relative positions of the macrocell users (MUs) and the FAPs. The MUs are classified as "femto-interfering users" that can use only some dedicated subcarriers, and "regular users" that can use both the dedicated subcarriers and the shared subcarrier which are also used by the femtocell

users. Secondly, an intra-tier interference mitigation strategy is developed by using an auction algorithm to optimize the subcarrier assignment for both the macrocell and the femtocell. As a result, the interference among FUs and MUs is mitigated and the whole network system throughput is maximized.

The remainder of this paper is organized as follows. Section II describes the uplink interference problem in femtocell networks. Section III proposes the inter-tier uplink interference mitigation strategy by dividing all MUs into two groups with partial cochannel spectrum deployment. Section IV develops the intra-tier uplink interference mitigation method among femtocells by means of subcarrier allocation which is optimized by an auction algorithm. Simulation results are presented in Section V. Finally, concluding remarks are given in Section VI.

II. Interference in femtocell networks

In a standard cellular system using OFDMA-based network access, frequency allocation must take into consideration both inter- and intra-cell interference. Each subcarrier should be allocated to only a single user within the cell (or sector) so that intra-cell interference is avoided. Moreover, users from adjacent cells (or sectors) might cause interference to the users in the cell of interest so frequency allocation has to be optimized to minimize the inter-cell interference.

With femtocells overlaying on top of a traditional cellular deployment, the complexity of the interference problem increases significantly and new mitigation strategies have to be designed. Assume that a femtocell network has a single MBS, then one can expect to encounter three types of uplink interference: MU to FAP interference, FU to MBS interference, and FU to FAP interference, as illustrated in Fig. 1.

A. MU to FAP Interference

In OFDMA-based systems such as mobile WiMax, power control is employed for the uplink [19]. It ensures that, at any time, a given MU is transmitting enough power to achieve a minimum signal-to-interference-plus-noise-ratio (SINR) at the MBS receiver given the current channel condition, which is measured by the system periodically.

If an MU is located far away from the MBS, the power control algorithm will set its transmitted power to a high level to meet the target SINR value. As depicted in Fig. 1(a), if an MU happens to be in the vicinity of a femtocell and also far away from the MBS, then its signal could be high enough to propagate through the walls of the building where the FAP is deployed and generate interference. This will happen only if the FU in the femtocell uses the same frequency as the MU. It is important to note that, as stated in [2], it is indeed on the macrocell edge where femtocells are most necessary and useful, so this kind of interference is expected to be very frequent.

B. FU to MBS Interference

Due to the frequency reuse among femtocells, it is possible that many FUs in different femtocells use the same subcarrier as an MU, thus they will interfere with the macrocell, as depicted in Fig. 1(b). In

order to overcome the interference from FUs to the MBS, the MBS measures the interfered subcarrier and applies the uplink power control on the MU, which will determine that it needs to transmit higher power in order to reach its target SINR at the receiver. This increase of the transmission power will worsen even more the MU to FAP interference problem described above.

C. Femtocell to Femtocell Interference

A femtocell is, by definition, located indoors, so interference occurs when adjacent femtocells use the same subcarriers. The interference level between non-adjacent femtocells is negligible, because any signal coming from one FU travels through at least two walls to reach the FAP of a non-adjacent femtocell. Therefore, the frequency allocation strategy should not allocate the same subcarriers in adjacent femtocells in order to avoid the intra-tier interference among femtocells.

III. Inter-tier Interference Mitigation with Partial Cochannel Assignment

An example of femtocells and macrocell coexistence in a two-tier network is illustrated in Fig. 2. The femtocells overlay on top of the macrocell forming a hierarchical cell structure. At distances D_1 and D_2 respectively from MBS, 25 surrounding femtocells are arranged in a square grid (e.g., residential neighborhood) of area $D^2 = 10000m^2$, with 5 femtocells per dimension [13], [20]. The radius of each femtocell is $R^{FC} = 10m$ [21]. The FAPs are located in the center of their corresponding femtocells. The coverage radius of the macrocell is $R^{MC} = 500m$. We assume that the inter-macrocell interference is mitigated through fractional frequency reuse (FFR) [18]. Therefore we focus on inter-tier interference mitigation under a single macrocell scenario.

Based on the fact that there are much less number of FUs in each femtocell than the number of MUs in each macrocell, a portion of the whole spectrum would be sufficient for femtocells in most cases [11]. Furthermore, in order to avoid performance degradation due to interference, it may be better to limit the spectrum that a femtocell can use, which is verified in section V. Therefore, it is reasonable to adopt the partial cochannel deployment strategy and to implement spectrum reuse among femtocells by means of subcarriers allocation. Given a total number of available subcarriers N, we assume that N_s subcarriers are shared by the FU and MUs, whereas the remaining $(N - N_s)$ subcarriers are used by MUs only. The transmitting power of MU is denoted as P^{MU} and $P^{MU}_{\min} \leq P^{MU} \leq P^{MU}_{\max}$ by using power control according to the measurement of each subcarrier channel state. Owing to the small radius of the femtocell and FU and MU being the same type of terminal, we assume that the transmission power of FU, P^{FU}, is constant and $P^{FU} = P^{MU}_{\min}$. It is shown that such constant power assignment on subcarriers will not bring noticeable rate decline compared to the mercury water-filling (MWF) power control algorithm in [22].

A. Inter-tier Interference Mitigation Strategy

In this subsection we propose a cochannel interference mitigation strategy between MUs and FUs over the shared subcarriers. We address the uplink interference problem by considering the QoS requirements

for both MU and FU in term of SINR. As for mitigating the interference from FUs to the MBS, the MU first uses power control to improve the SINR in order to satisfy its QoS requirement. If the MU cannot reach its minimum SINR requirement due to the long distance from the MBS and the interference from FUs, it should switch to the dedicated subcarriers. If the MU can meet its target SINR, then it will be checked whether or not its transmission power is strong enough to interfere with its nearest cochannel FU. If the position of the MU is close enough to an FAP to interfere with the cochannel FU, it should use the dedicated subcarriers. The proposed strategy for eliminating the inter-tier interference (i.e., MU to FAP and FU to MBS) is summarized as follows.

- For any given MU m, estimate the total path loss to the MBS (χ_m^{MU}) and estimate the path loss to its closest active FAP (χ_m^{MF}) by measuring the Reference Signal Received Power (RSRP) of the active FAPs in the downlink [11].
- Check whether the MU can meet its target SINR by using power control. If yes, consider the worst interference case from this MU to its nearest FAP, where the FU is on the edge of this FAP. Then the MU estimates whether or not its transmission power causes the FU 's SINR below the minimum requirement. Here, the reason for considering the worst case scenario is to maintain the uplink coverage of the femtocell.
- If both the MU and the FUs in its closest femtocells can satisfy their SINR requirements, the MU is a regular user and can use either the shared subcarriers or the dedicated subcarriers. Otherwise, the MU is a femto-interfering user and can only use the dedicated subcarriers.

After the above strategy is applied, all MUs within the macrocell are classified as either "regular users" or "femto-interfering user." Such classification of MUs depends on many system parameters, such as the macrocell radius, femtocell radius, penetration loss through the building wall, transmission power of an FU, etc. We next describe the classification procedure in detail.

B. Classification of MUs

In order to make sure that the MUs do not interfere any FU in the closest femtocell, we should consider the worst case scenario that an FU is at the edge of the femtocell. Assume that the estimated distance from the MU to the closest FAP d^{MF} is obtained by the RSRP measurement from the FAP in the downlink. Based on the value of RSRP and the FAP transmission power which is set to be constant in partial cochannel deployment, the MU can calculate the path loss from the FAP to it, then the distance from the MU to its closest FAP can be estimated according to the path loss model. Then the interference from the MU to the FAP is given by

$$I^{MF} = \frac{P^{MU} G^F G^U}{\chi^{MF}} \tag{1}$$

where P^{MU} is the transmit power of the MU, G^F is the antenna gain of the FAP, and χ^{MF} is the path loss from the MU to the FAP and is related to d^{MF}. G^U is the antenna gain of MU which is also the

antenna gain of FU since both MU and FU are the same type of terminals.

As for the interference from FUs in other femtocells to this FU, after applying the auction algorithm for the shared subcarrier allocation to be described in the next section, the interference between adjacent femtocells can be avoided. Then the worst case scenario is shown on the right-hand side of Fig. 2, where the femtocells with the same color use the same subcarrier and interfere with each other. We analyze the interference from FUs in FAPs 3, 11, 15 and 23 to the FU in FAP 13 with the interfering FUs located at the closest positions to FAP 13. The interference from FUs in the outer rings is ignored due to the long distance and extra penetration losses through walls. Then, the sum interference from FUs in FAPs 3, 11, 15 and 23 to the FU in FAP 13 is given by

$$I^{FF} = \frac{4P^{FU}G^{F}G^{U}}{\chi^{FF}} \tag{2}$$

where χ^{FF} accounts for the path loss from one of the interfering FUs to FAP 13 as shown on the right-hand side of Fig. 2 and can be calculated using the distance of $3R^{FC}$. G^{F} is the antenna gain of FAP.

The interference from FUs to the MU is given by

$$I^{FM} = \sum_{i \in \mathcal{M}_{\text{int}}} \frac{P^{FU}G^{M}G^{U}}{\chi_{i}^{FM}} \tag{3}$$

where $\mathcal{M}_{\text{int}}$ indicates the set of interfering FUs to the MU, and χ_{i}^{FM} is the path loss from the ith FU in $\mathcal{M}_{\text{int}}$ to the MBS.

Under the worst case interference scenario described above, the SINRs of the MU and the FU still have to satisfy the following constraints

$$\gamma^{FU} = \frac{P^{FU}G^{F}G^{U}/\chi^{FU}}{I^{MF} + I^{FF} + W} \geq \gamma_{\min}^{FU} \tag{4}$$

$$\text{and} \gamma^{MU} = \frac{P^{MU}G^{M}G^{U}/\chi^{MU}}{I^{FM} + W} \geq \gamma_{\min}^{MU} \tag{5}$$

where W accounts for the noise power; χ^{FU} and χ^{MU} denote the path loss from the FU to its FAP, and that from the MU to MBS, respectively; $\gamma_{\min}^{FU}$ and $\gamma_{\min}^{MU}$ are the minimum SINR requirements for the MU and FU, respectively. The MU can measure and report uplink SINR, then the MBS can acquire the value of γ^{MU}. γ^{FU} can be estimated by MBS according to the transmission power of MU and the path loss from the MU to its nearest FAP.

Taking equalities in (4) and (5), and using (1)-(3), we can solve for χ^{MU} and obtain

$$\chi_{\max}^{MU} = \frac{\chi^{MF}G^{M}(\frac{P^{FU}G^{U}}{\gamma_{\min}^{FU}\chi^{FU}} - \frac{I^{FF}+W}{G^{F}})}{(I^{FM}+W)\gamma_{\min}^{MU}} \tag{6}$$

where $\chi_{\max}^{MU}$ is the maximum path loss from MU to its MBS with the constraints of (4) and (5). All the parameters on the right-hand side of (6) are constants except for the two variables χ^{MF} and I^{FM}. Thus, $\chi_{\max}^{MU}$ is primarily affected by the path loss from the MU to its closest FAP, χ^{MF}, and the interference

from the FUs to the MBS, I^{FM}. As for I^{FM}, due to the frequency reuse among femtocells, its value is mainly related to the minimum distance from FUs to the MBS and the active probability of femtocells, which varies much slower than χ^{MF}. Therefore, different MUs have different $\chi^{MU}_{\max}$ due to their different locations. The MU with a larger distance from its closest FAP will have a larger $\chi^{MU}_{\max}$. Any MU whose path loss to the MBS is less than its corresponding $\chi^{MU}_{\max}$ will be classified as a regular user and it can use either the dedicated subcarriers or the shared subcarriers. The others will be classified as femto-interfering users and they can only use the dedicated subcarriers. An intuitive way to understand the above MU classification scheme is by defining $d_{\max}$ as the distance where a given MU will suffer a total path loss of $\chi^{MU}_{\max}$. Any MU laying within $d_{\max}$ can use any subcarriers, whereas any MU located outside of $d_{\max}$ can only use the dedicated subcarriers. In this way, both the MU and FU can meet their target SINR requirements and therefore the inter-tier interference is avoided. Note that the actual value $d_{\max}$ is not a constant value and depends on the current values of path loss and the distance from this MU to its nearest cochannel femtocell, d^{MF}.

C. Path Loss Model

The path loss model based on suburban deployment in [20] is used in this paper. Assume that the FAPs are located in single-floor houses/buildings.

1) Indoor link (FU to FAP)

- FU to FAP, FU is inside a different house with FAP

$$\chi = \max(15.3 + 37.6\log_{10}d,\ 38.46 + 20\log_{10}d) + 0.7d_{indoor} + n_w L_w + X \tag{7}$$

- FU to FAP, FU is inside the same house with FAP

$$\chi = 38.46 + 20\log_{10}d + 0.7d_{indoor} + X \tag{8}$$

2) outdoor link (MU to MBS)

$$\chi = 15.3 + 37.6\log_{10}d + X \tag{9}$$

3) outdoor-to-indoor link (MU to FAP and FU to MBS)

$$\chi = \max(15.3 + 37.6\log_{10}d,\ 38.46 + 20\log_{10}d) + 0.7d_{indoor} + L_w + X \tag{10}$$

where d is the transmitter-receiver separation in meters; d_{indoor} is the indoor distance in meters; L_w is the penetration loss through external walls, generally assumed to be 15dB [9]; n_w is the number of penetrated walls. Using an intra-tier interference mitigation scheme among femtocells (see next section) we can assume $n_w \geq 2$ for the path loss χ^{FF}. As for the shadow fading X(dB), a general normal

distribution with a standard deviation of 4dB is used for the FU to FAP with FU being inside the same house with the FAP, otherwise a standard deviation of 8dB is used.

IV. Intra-tier Interference Mitigation via Auction-based Subcarrier Assignment

As discussed in the previous section, the cochannel interference from FUs to MBS is avoided by using uplink power control on MUs. Based on the power control results, all MUs are classified as "regular users" and "femto-interfering users". By allocating only dedicated subcarriers to femto-interfering users, inter-tier interference is mitigated and both the MUs and FUs can meet their target SINR requirements if the intra-tier interference can also be eliminated, which can be achieved by independently allocating subcarriers for macrocells and femtocells, as discussed in this section.

A. Macrocell Subcarrier Allocation

The power control algorithm requires that the system measures the channel states between the MBS and the MUs periodically. After each measurement the system recalculates the current value of $\chi_{\max}^{MU}$ and classifies each MU as a regular user or a femto-interfering user.

Consider a single macrocell system with an MBS and M MUs. Assume that each subcarrier can only be assigned to one user. Denote F_s as the set of shared subcarriers and F_d as the set of dedicated subcarriers. Further denote U_{reg} as the set of regular users and U_{int} as the set of femto-interfering users. Let a_{mn}^{MU} be an indicator variable such that $a_{mn}^{MU} = 1$ if the nth subcarrier is allocated to the mth MU, otherwise $a_{mn}^{MU} = 0$. Suppose that the mth MU requires to be allocated k_m subcarriers. Note that we should have $\sum\limits_m k_m \leq N$. Then, given a priority or weighting factor ω_m for the mth MU, the macrocell subcarrier allocation problem can be formulated as follows:

$$\begin{aligned} \max_{\{a_{mn}^{MU}\}} \quad & \sum_{m=1}^{M} \omega_m \left(\sum_{n=1}^{N} c_{mn}^{MU} a_{mn}^{MU} \right), \\ \text{s.t.} \quad & a_{mn}^{MU} \in \{0,1\}, \\ & \sum_m a_{mn}^{MU} \leq 1, \ \ \forall n, \\ & \sum_n a_{mn}^{MU} = k_m, \ \ \forall m, \\ & a_{mn}^{MU} = 0, \ \ \forall n \in F_s, \forall m \in U_{int}. \end{aligned} \tag{11}$$

The second constraint indicates that any subcarrier can be allocated to at most one MU to avoid intra-cell interference. The third one defines that the number of subcarriers allocated to an MU. The third one defines that the number of subcarriers allocated to an MU, where $\tilde{k}_{ml} \leq k_m \leq \tilde{k}_{mu}$. $\tilde{k}_{ml}$ and $\tilde{k}_{mu}$ are respectively the minimum and maximum numbers of subcarriers allocated to MU m, for all $1 \leq m \leq M$ such that $\sum_{m=1}^{M} \tilde{k}_{ml} < N$. In order to guarantee the fairness among MUs, all subcarriers are evenly allocated to all the MUs. Finally, the last one prevents the femto-interfering MUs from occupying the shared subcarriers.

c_{mn}^{MU} denotes the data rate for MU m on subcarrier n. If the nth subcarrier for MU m has SINR γ_{mn}^{MU}, assuming a 3dB gap to theoretical rate [23], then its rate can be estimated as

$$c_{mn}^{MU} = \log(1 + \gamma_{mn}^{MU}/2) \ \text{(bits/channel use)} \tag{12}$$

Note that here the SINR values can be measured and reported by MU to the MBS.

The optimization problem given by (11) can be translated into a special 0-1 combinatorial optimization problem by introducing a dummy user with index $m = 0$, such that $c_{0,n}^{MU} = 0, \ \forall n$, and the number of its allocated subcarriers $k_0 = N - \sum_{m=1}^{M} k_m$, with the understanding that any subcarrier assigned to the dummy user is not used for data transmission. The mth user is divided into k_m "subusers" and an indicator variable $\tilde{a}_{m,l,n}^{MU}, l = 1, 2, \cdots, k_m$ is defined such that $\tilde{a}_{m,l,n}^{MU} = 1$ if the nth subcarrier is allocated to the lth subuser of the mth user. In addition, let $\tilde{w}_{m,l} \triangleq w_m$ and $\tilde{c}_{m,l,n}^{MU} \triangleq c_{mn}^{MU}, \ l = 1, 2, \cdots k_m$. Thus the original optimization problem (11) is converted to the following

$$\begin{aligned}
\max_{\{\tilde{a}_{m,l,n}^{MU}\}} \quad & \sum_{m=0}^{M} \sum_{l}^{k_m} \tilde{\omega}_{m,l} \left(\sum_{n=1}^{N} \tilde{c}_{m,l,n}^{MU} \tilde{a}_{m,l,n}^{MU} \right), \\
\text{s.t.} \quad & \sum_{m} \sum_{l} \tilde{a}_{m,l,n}^{MU} = 1, \ \ \forall n, \\
& \sum_{n} \tilde{a}_{m,l,n}^{MU} = 1, \ \forall m, l, \\
& \tilde{a}_{m,l,n}^{MU} = \{0, 1\}, \\
& \tilde{a}_{m,l,n}^{MU} = 0, \ \ \forall n \in F_s, \forall m \in U_{int},
\end{aligned} \tag{13}$$

which is a symmetric assignment problem. It is shown in [22] that such an assignment problem can be solved efficiently using the auction algorithm which has a very low computational complexity and memory requirement. We next extend the auction algorithm in [22] to solve our problem (13) with more constraints for the subcarriers allocation for MUs in the macrocell.

The auction algorithm is an intuitive method for solving the assignment problem. It mimics a competitive bidding process in which unassigned players raise their prices and bid for objects simultaneously. Assuming a set of prices $\{r_n, n = 1, \cdots, N\}$, being N the total number of objects, and a positive scalar ε, a player m is defined as happy with the object n_m if the profit (i.e., reward minus price) of assigning this object to itself is within ε from the optimal, i.e.,

$$f_{mn_m} - r_{n_m} \geq \max_{n} \{f_{mn} - r_n\} - \varepsilon, \tag{14}$$

where f_{mn_m} denotes the reward of object n_m to player m and r_{n_m} represents the current price of object n_m. If the assigned object n_m to player m cannot satisfy the inequality (14), the player is defined as unhappy. For problem (13), the reward is the data rate of each subcarrier for every subuser and the price is an increasing variable which is proportional to the data rate during the auction process. The subcarrier price update procedure is given in Algorithm 1, which is the detailed auction algorithm for solving (13). The condition (14) is known as ε-complementary slackness. Without ε, when more than one subcarrier achieve the maximum value for one MU, the price of subcarrier $n_{m,l}$ will not increase, thereby causing

never-ending iterations [22], [24]. The number of iterations needed to converge to an assignment scheme in Algorithm 1 proportional to C/ξ, where $C = \max_{m,l,n} f_{m,l,n}$.

Algorithm 1: The auction algorithm for macrocell subcarrier allocation.

1. **Initialization**: Select ε and set all subusers as unhappy except for the dummy subusers. Every subuser estimates the reward for each subcarrier, i.e., $f_{m,l,n} = \tilde{c}^{MU}_{m,l,n}$. Set every subcarrier price $r_n = 0, n = 1, \ldots N$.

2. **Repeat**

a) Choose an unhappy femto-interfering subuser from U_{int}, calculate its maximum profit $\varphi_{m,l,n_{m,l}} = \max_n(f_{m,l,n} - r_n)$ and the second maximum profit $\phi_{m,l,\bar{n}_{m,l}} = \max_{n,n\neq n_{m,l}}(f_{m,l,n} - r_n)$ from dedicated subcarriers.

b) Allocate subcarrier $n_{m,l}$ to subuser (m, l). If this subcarrier has already been allocated to another femto-interfering subuser $(\bar{m}, \bar{l})$, remove that allocation. Further, if subuser (m, l) has been assigned an subcarrier before, allocate that subcarrier to subuser $(\bar{m}, \bar{l})$.

c) Update the price of the subcarrier $n_{m,l}$ as $r_{n_{m,l}} = r_{n_{m,l}} + (\varphi_{m,l,n_{m,l}} - \phi_{m,l,\bar{n}_{m,l}}) + \varepsilon$.

d) Set subuser (m, l) as happy. Decide whether subuser $(\bar{m}, \bar{l})$ is happy or not with its current allocation by checking (14).

3. **Until** all femto-interfering subusers are happy.

4. Allocate the remaining subcarriers to the regular unhappy subusers following Steps 2-3, until all regular subusers are happy.

5. Allocate the remaining subcarriers randomly to the dummy subusers.

As analyzed in [22], for any arbitrarily fixed ε, Algorithm 1 converges to an allocation that yields a total reward within $N\varepsilon$ from the optimal objective function value of (13). A larger ε produces a worse approximation to the optimal allocation but faster convergence; while a smaller ε results in a better approximation to the optimal allocation but slower convergence. After the MBS has allocated subcarriers, the cell is configured, and it is ready to transmit data. Periodically the MBS updates the femto-interfering user set and the regular user set, and monitors the channel quality of the subcarriers, then updates the subcarrier allocation.

B. Asynchronous Distributed Femtocell Subcarrier Allocation

Since each femtocell is not aware of the subcarrier allocation of either the macrocell or the other femtocells, the femtocell subcarrier allocations need to be carried out in a distributed fashion, based on the interference estimation on every subcarrier by using the "network listen" capability (sniffer) [25]. As discussed in Section III, the interference caused by a given FU to the non-neighboring FAP can be ignored. Therefore the distributed subcarrier allocation strategy should be devised to avoid adjacent

femtocells occupying the same subcarrier. The algorithms proposed in the following for intra-tier interference mitigation are intend to avoid adjacent femtocells occupying the same subcarriers. These algorithms assume that the number of shared subcarriers are sufficient enough for adjacent femtocells not occupying the same subcarriers and implementing the frequencies reuse among non-adjacent femtocells.

Similar to the macrocell subcarrier allocation, each femtocell is considered as a single cell system with a base station and P active FUs. We first consider a simple approach to distributed femtocell subcarrier allocation where each femtocell independently implements an auction algorithm for subcarrier allocation. But different femtocells operate asynchronously. In particular, we assume that each iteration of the subcarrier allocation update is performed every $t + \Delta t$ seconds in each femtocell, being Δt a random backoff time uniformly distributed. Considering one subcarrier allocated for a femtocell, in general, if it is also occupied by the adjacent femtocells, its SINR will be worse than the subcarriers not occupied by adjacent femtocells. As a result, the subcarriers already used in the adjacent femtocells are likely not to be allocated to the femtocell under consideration, and thus the interference among femtocells can be avoided.

Let p denote the pth user in the femtocell. Given a priority or weighting factor ω_p for this user, the subcarrier allocation over the shared subcarriers in the femtocell is formulated as follows:

$$\begin{aligned} \max_{\{a_{pn}\}} \quad & \sum_{p=1}^{P} \omega_p \left(\sum_{n=1}^{N_s} c_{pn} a_{pn} \right), \\ \text{s.t.} \quad & a_{pn} \in \{0,1\}, \ \ \forall p, n, \\ & \sum_{p} a_{pn} \leq 1, \ \ \forall n, \\ & \sum_{n} a_{pn} = k_p, \ \ \forall p, \end{aligned} \tag{15}$$

where c_{pn} denotes the obtainable throughput for the pth FU in the femtocell on the nth subcarrier and can be estimated in a similar way as in (12). The SINR on every subcarrier can be estimated by performing the interference measurement on every subcarrier by FAPs using the sniffer capability [25]. a_{pn} is also an indicator variable, such that $a_{pn} = 1$ if the nth subcarrier is allocated to the pth FU in the femtocell. The second constraint indicates that one given frequency can be allocated to at most one FU in the same femtocell to avoid intra-cell interference and the third one defines that the number of subcarriers one FU can be allocated to is k_p, where $\tilde{k}_{pl} \leq k_p \leq \tilde{k}_{pu}$. $\tilde{k}_{pl}$ and $\tilde{k}_{pu}$ are the minimum and maximum numbers of subcarriers allocated to the FU p respectively, for all $1 \leq p \leq P$ such that $\sum_{p=1}^{P} \tilde{k}_{pl} < N_{femto}$. N_{femto} is the number of subcarriers that each femtocell can occupy. In order to avoid adjacent femtocells occupying the same subcarriers for the 5×5 Grid Model shown in Fig. 2, we set $N_{femto} = \frac{1}{4} N_s$. In order to guarantee the fairness among FUs, all the subcarriers are evenly allocated among all the FUs in each femtocell. Similarly as in Section IV.A, this optimization problem can be easily translated into a symmetric assignment problem by introducing dummy users and can be solved efficiently using the auction algorithm. Independently and asynchronously, the FAPs also periodically estimate the quality of

the allocated subcarriers and update the subcarrier allocation if necessary.

C. Distributed Joint Femtocell Subcarrier Allocation

In this subsection we consider joint subcarrier allocation among all femtocells within the macrocell. Note that the resulting algorithm is much more complex than the one from the previous subsection, in that it involves message exchange between adjacent femtocells during each iteration. It will be shown in Section V that the simple asynchronous and independent allocation scheme actually performs similarly to this more complex joint allocation scheme. Hence the method presented here eventually is only used as a benchmark for comparison purpose.

Note that the inter-femtocell interference is mainly caused by the adjacent femtocells. The received signal power from non-adjacent femtocells is very low due to twice the wall penetration loss, and thus is negligible. Hence the subcarrier allocation scheme should avoid allocating the same subcarriers to adjacent femtocells. We introduce "virtual" users to capture the interaction between adjacent femtocells. Every FU in a femtocell generates a virtual user at each adjacent femtocell. Each virtual user is allocated the same subcarriers as its corresponding FU. This way, the multicell subcarrier allocation problem can be decomposed into a group of single cell frequency allocation problems in which the interference between users in different femtocells is represented by constraints between its own users and the corresponding virtual users.

Let $\mathcal{S}_q$ represent the q-th femtocell's interference user set containing all the users in its adjacent femtocells, such that every user $p_{i,i\neq q} \in \mathcal{S}_q$ can generate interference to the qth femtocell. Let $\tilde{p}_{iq}$ denote the virtual user generated for the qth femtocell by the FU p_i in the adjacent ith femtocell. Then, the optimization of multi-femtocell subcarrier allocation problem can be formulated as follows.

$$\begin{aligned}
\max_{\{a_{p_q n}\}} \quad & \sum_{q=1}^{Q}\sum_{p_q=1}^{P} \omega_{p_q n}\left(\sum_{n=1}^{N_s} c_{p_q n} a_{p_q n}\right), \\
\text{s.t.} \quad & a_{p_q n} \in \{0,1\}, \ \ \forall p_q, q, n, \\
& \sum_{p_q} a_{p_q n} + \sum_{p_i \in \mathcal{S}_q} a_{\tilde{p}_{iq} n} \leq 1, \ \ \forall q, n, \\
& \sum_{n} a_{p_q n} = k_{p_q}, \ \ \forall p_q, q, \\
& a_{\tilde{p}_{iq} n} = a_{p_i n}, \ \ \forall n, p_i \in \mathcal{S}_q, q.
\end{aligned} \tag{16}$$

The first three constraints are equivalent to those for the single-cell case in (15). The fourth constraint models the effect of inter-femtocell interference. Note that the problem in (16) is feasible if and only if $\sum_{p_q} k_{p_q} + \sum_{p_i \in \mathcal{S}_q} k_{p_i} \leq N_s$. Further, due to the coupling of subcarrier allocation between the femtocells, it is nontrivial to obtain a good feasible solution via a low-complexity distributed approach.

We extend the greedy algorithm proposed in [22] to solve this problem. In the first step, the auction method is independently performed for resource allocation in every femtocell ignoring the constraint that each user and its corresponding virtual user(s) must share the same resource. The reward for allocating a

subcarrier in a cell to any of its users is acquired based on the channel state measurement and network sniffer capability, while the reward for allocating a subcarrier in a cell to any virtual user is set as zero in the first step, so no cell will allocate any resource to its virtual users. In the second step we ensure that every user occupies the same subcarriers as its corresponding virtual user(s), by trading subcarriers in a greedy fashion. The detailed procedure is summarized in Algorithm 2.

Algorithm 2: The auction algorithm for multi-femtocell joint subcarrier allocation.

1. Initialization: Obtain the set $\mathcal{S}_q$ for each femtocell q.

2. Run the auction algorithm to perform subcarrier allocation for every single femtocell.

3. **For** the qth femtocell, where $1 \leq q \leq Q$

a) Collect the subcarrier allocation results for each user in $\mathcal{S}_q$ and femtocell q, and acquire the conflicting subcarriers which are simutaneously occupied by the users in $\mathcal{S}_q$ and femtocell q. Let $\mathcal{C}_q$ denote the set including all the conflicting subcarriers.

b) **For** each conflicting subcarrier in femtocell

1) If the weighted rate of the assigned user in cell q is less than that of any user in $\mathcal{S}_q$, then remove the subcarrier from the allocated user in femtocell q. Find the maximum weighted rate subcarrier from the remaining subcarriers which are not occupied by the femtocell q and the users in $\mathcal{S}_q$, then allocate this subcarrier to this user in femtocell q.

2) Otherwise, remove the subcarrier from all the users in $\mathcal{S}_q$, and find the maximum weighted rate subcarrier for each user from their corresponding remaining subcarriers which are not allocated to the users in its corresponding femtocell and interference user set.

3) Pass the updated subcarrier allocation result of each user in $\mathcal{S}_q$ to its serving FAP.

c) **End for**

4. **End for**

V. Simulation Results

Simulation results are presented in this section for the setup of Fig. 2. First, $d_{\max}^{MU}$, which is used to classify whether an MU is a regular user or a femto-interfering user, is simulated under different modulation formats. Second, the performance of our proposed inter-tier and intra-tier interference mitigation schemes under partial cochannel deployment is compared with other methods.

We assume that the femtocell occupies one quarter of the total subcarriers. In each snapshot, the number of FUs in each femtocell is 4 and within a femtocell they are uniformly distributed with a minimum distance of $2m$ from their corresponding FAP. One quarter of the MUs are deployed following a uniform distribution in a distance range of $20m - 220m$ from MBS which mainly produce interference to the FUs in the near square grid. The other three quarters of MUs are positioned randomly in a distance range of $300m - 500m$ from MBS which primarily interfere with the FUs in the far square grid.

A multipath Rayleigh fading channel with a Doppler spread that models pedestrian users moving at a speed of $v = 1.5m/s$ is considered for the subcarrier data rate calculation in subcarrier allocation. The multipath profile for indoor propagation is extracted from the model B in [26], with a delay spread of $100ns$ for indoor and $45ns$ for outdoor. Assume that the system can transmit with all possible modulations in WiMax-OFDMA (i.e., QPSK, 16-QAM and 64-QAM) [27]. The minimum required SINRs for all these modulations with a $\mathrm{BER} = 10^{-6}$ are listed in II. The levels of minimum SINR requirement that we use in our work are extracted from the Mobile WiMAX standards and they guarantee a probability of error of 10-6, which is more than enough to provide all kinds of QoS and services. The rest of the system parameters for the base stations and the mobile terminals are listed in Table I.

A. Analysis of $d_{\max}^{MU}$

Recall that whether an MU is a regular user or a femto-interfering user is based on its corresponding $d_{\max}^{MU}$, which is mainly related to the distance from the MU to its nearest FAP, d^{MF}. If this value is high enough, the MU transmitting high power still cannot create much interference to the FAP [Fig. 1(a)] due to the large path loss from the MU to this femtocell, so it will increase the value of $d_{\max}^{MU}$. Note that only the large scale fading is considered and shadowing and multipath fading are omitted here. Fig. 3 depicts the value of $d_{\max}^{MU}$ as a function of different values of d^{MF}, under three modulations. It is seen that, with the same d^{MF}, the largest $d_{\max}^{MU}$ corresponds to the QPSK modulation. When an MU is 30 meters away from its closest FAP in QPSK mode, its $d_{\max}^{MU} = 500m$, which means that this MU can be classified as regular user even though it locates on the edge of the macrocell. Note that $d_{\max}^{MU}$ increases monotonously with the distance d^{MF} due to the decreasing interference caused to the FAP from MUs.

B. Performance Analysis for FUs and MUs

We consider the following two proposed schemes for inter-tier and intra-tier interference mitigation under partial cochannel deployment.

(1) Prop.1: MUs are first classified as regular and femto-interfering users and then Algorithm 1 is employed for macrocell subcarrier allocation. Independent and asynchronous subcarrier allocation is performed for femtocells over the shared subcarriers.

(2) Prop.2: Same as Prop.1 for MUs in the macrocell. Joint subcarrier allocation is performed for femtocells (i.e., Algorithm 2) over the shared subcarriers.

We compare the above two proposed schemes with the following methods.

- Random allocation: The subcarriers are allocated randomly in the macrocell and femtocell under the partial cochannel deployment.
- No MU part., indep. femto: All MUs can use any subcarrier and the macrocell subcarrier allocation is performed by using the auction algorithm. Independent and asynchronous subcarrier allocation is performed for femtocells over shared subcarriers.

- No MU part., joint femto: All MUs can use any subcarrier and the macrocell subcarrier allocation is performed by using the auction algorithm. Joint subcarrier allocation is performed for femtocells over shared subcarriers.
- Cochannel demployment: All MUs and FUs can use any subcarrier. Subcarrier allocation in macrocell and femtocells are performed independently and asynchronously using the auction algorithm.
- Orthogonal deployment: MUs just occupy the dedicated subcarriers and FUs only use the shared subcarriers. The subcarriers are allocated among MUs by using the auction algorithm, and among FUs by using the auction algorithm independently and asynchronously. .

The following simulation results are averaged over 200 network realizations. In general, not all the 50 femtocells are active at any time, and those with no FUs transmitting in their coverage will be idle. We define the femtocell active probability as the ratio between the number of active femtocells and the total number of femtocells in the network. In the simulation, the femtocell active probability ranges from 0.6 to 1.

1) Spectral Efficiency and Throughput Comparison: Assume that the total bandwith is B Hz, then the bandwith for each subcarrier is B/N Hz. Let the duration of one OFDMA symbol be T seconds. Then $1\ channel\ use = (B/N)T$. Denote the rate of the nth subcarrier for user m as c_{mn}, the spectral efficiency of subcarrier n for user m is then

$$\frac{c_{mn}}{TB/N} = \frac{Nc_{mn}}{TB} \quad \text{bits/s/Hz.}$$

Given the subcarrier allocation results $\{a_{mn}\}$, then the throughput over all the allocated subcarriers is

$$\sum_{m=1}^{M}\sum_{n=1}^{N} \frac{c_{mn}a_{mn}}{T} \quad \text{bits/s.} \tag{17}$$

The CDFs (cumulative distribution function) of the spectral efficiencies of the FUs under different schemes are shown in Fig. 4. The spectrum efficiency of every FU is defined as the average spectrum efficiency of the subcarriers allocated to FUs. The spectral efficiencies are collected under different femtocell activity probabilities as used in Fig. 5, which shows the average femtocell throughput as a function of the femtocell active probability. From Fig. 4 and Fig. 5, one can see that the performance of Prop.1 and Prop.2 is very close to that of orthogonal deployment, which has the best FU spectral efficiency and throughput due to its complete interference avoidance from MUs. In Prop.2, the coupling effect is considered among adjacent femtocells which can more efficiently avoid adjacent femtocells occupying the same subcarrier, so its performance is slightly better than that of Prop.1. As for the schemes of No MU part., indep. femto and No MU part., joint femto, because the inter-tier interference mitigation strategy is not employed, the uplink interference from MUs to FAPs is strong, thus the FU spectral efficiency and femtocell throughput are worse than our proposed methods. As for the Cochannel deployment, due to the more available subcarriers than other methods, it has more opportunities to select better subcarriers which have better channel states. The interference among femtocells can be decreased, so

the percentage of FUs with large value of spectral efficiency is higher than other method. While, without inter-tier interference mitigation strategy, it still have sever interference from MUs. The percentage of FUs with low spectral efficiency is larger than that of Prop.1 and Prop.2. Moreover, the performance of Random allocation is the worst.

Fig. 6 shows the CDF of the spectral efficiency of MUs and Fig. 7 depicts the macrocell throughput versus the femtocell active probabilities. The spectrum efficiency of every MU is defined as the average spectrum efficiency of the subcarriers allocated by MUs. From Fig. 6, the best performance method is orthogonal deployment in terms of the MU spectral efficiency, due to the complete interference avoidance from femtocells. However, the available subcarriers for MUs are only just $3/4$ of all the subcarriers owing to allocating $1/4$ of the subcarriers to femtocells in orthogonal deployment, so the macrocell throughput drops significantly compared to our partial cochannel deployment and cochannel deployment as shown in Fig. 7. Note that although the orthogonal deployment method has the highest spectral efficiency, since $1/4$ the of subcarries are reserved for femtocell users, the macrocell throughput is decreased. Compared with the schemes of No MU part., indep. femto and No MU part., joint femto, our proposed methods (Prop.1 and Prop. 2) prevent the femto-interfering MUs from occupying the shared subcarriers, which results in slightly MU performance degradation but FU performance improvement. Note that in the 5-percentile in Fig. 6, the throughput is not improved noticeably using the auction algorithm. This is because we set the weighting factors to be the same for all macrocell users, and some edge users may be starved . However, this situation can be improved by increasing the weighting factors for the edge users at the sacrifice of the overall system throughput.

2) Collision Probability among Femtocells: If two adjacent femtocells occupy the same subcarrier, we call it a collision event. Then the ratio between the number of the colliding subcarriers and the total allocated subcarriers in the femtocells is defined as the collision probability. In order to verify that the adjacent femtocells can avoid occupying the same subcarrier by using independent and asynchronous subcarrier allocation and joint subcarrier allocation, the subcarrier allocation collision probability among femtocells is shown in Fig. 8 as compared with random subcarrier allocation. We consider the scenario in Fig. 2 without MUs, then the subcarriers are just allocated among femtocells. It is seen that random allocation algorithm has the highest collision probability; and the independent and asynchronous subcarrier allocation algorithm is just slightly worse than the joint subcarrier allocation.

3) Outage Probability of MU and FU: The outage probability of MU and the FU versus the femtocell active probability is shown in Fig. 9. An outage occurs when the SINR of a subcarrier is below the target outage threshold, which is assumed to be 5dB lower than the target SINR threshold in the power control. The ratio between the number of subcarriers under the target outage threshold and the number of total subcarriers is the outage probability. Due to the fact that MUs and FUs use a different set of subcarriers in the orthogonal deployment, the inter-tier interference is avoided completely at the expense of sacrificing the available subcarriers for the MUs. Under this strategy the outage probabilities of MU and FU are

the smallest. The random allocation is the worst for both MUs and FUs. The MU outage probability for the proposed methods Prop.1 and Prop.2 do not drop noticeably due to the femto-interfering MUs being prevented from using the shared subcarriers. Independent and asynchronous subcarrier allocation and joint subcarrier allocation hardly affect the MU outage probability, because the interference from FUs to MBS is very low owing to the small transmission power of FUs, large path loss and the penetration losses. After using the auction algorithm in the macrocell, the MU outage probability of MU is reduced by nearly 50% compared to the random allocation. With an increasing number of active femtocells, the inter-tier interference from FUs to MBS increases, as a result, the MU outage probability of MU increases accordingly. Owing to the wall penetration loss, the SINR of FU is better than that of MU, so the FU outage probabilities of FU stay quite low. While the random allocation still has the highest FU outage probability, the FU outage probabilities of our proposed schemes are nearly zero as shown in Fig. 9(b).

4) Convergence of the Proposed Algorithms: The convergence of Algorithm 1 for macrocell subcarrier allocation and the independent and asynchronous subcarrier allocation algorithm for femtocell subcarrier allocation are shown in Fig. 10. It is seen from Fig. 10(a) that in Algorithm 1, after 6 iterations the average spectrum efficiency of MU converges to a stable value. As for the independent and asynchronous subcarrier allocation algorithm, after 4 iterations the average spectrum efficiency of FU converges to a stable value, as shown in Fig. 10(b). Hence the proposed methods have fast convergence.

VI. Conclusions

In this paper, we have proposed interference mitigation strategies for OFDMA-based femtocell networks, consisting of a conventional macro cellular deployment and overlaying femtocells. The proposed solution is composed of two components. The first is an inter-tier interference mitigation strategy that can be applied to a partial cochannel assignment, which divides all the macrocell users into femto-interfering users, which can only use the dedicated subcarriers, and regular users, which can use either dedicated subcarriers or the shared subcarriers. The femtocell users use only shared subcarriers. The second component consists of auction-based subcarrier allocation algorithms for the macrocell and femtocells, respectively, for mitigating intra-tier interference and maximizing the throughput. These algorithms have low computational complexity and memory requirement, and they run independently and asynchronously in each macrocell and femtocell. Extensive simulation results have demonstrated that the proposed interference mitigation framework can effectively mitigate both inter-tier and intra-tier interference and improve the overall network throughput of both the macrocell and femtocells.

References

[1] G. Mansfield, "Femtocells in the US market -business drivers and consumer propositions," in *FemtoCells Europe*, 2008, pp. 1927–1948.

[2] V. Chandrasekhar and J. G. Andrews, "Femtocell networks: A survey," *IEEE Commu. Mag.*, vol. 46, no. 9, pp. 59–67, Sept. 2008.

[3] S. Yeh, S. Talwar, S. Lee, and H. Kim, "WiMAX femtocells: a perspective on network architecture, capacity, and coverage," *IEEE Commu. Mag.*, vol. 46, no. 10, pp. 58–65, Oct. 2008.

[4] V. Chandrasekhar and J. Andrews, "Spectrum allocation in tiered cellular networks," *IEEE Commu. Mag.*, vol. 57, no. 10, pp. 3059–3068, Oct. 2009.

[5] D. Lopez-Perez, A. Valcarce, and G. de la Roche, "OFDMA femtocells: A roadmap on interference avoidance," *IEEE Commu. Mag.*, vol. 47, no. 9, pp. 41–48, Oct. 2009.

[6] M. Neruda, J.Vrana, and R. Bestak, "Femtocells in 3G mobile networks," in *Proc. IEEE Int. Conf. on System, Sigal and Image Processing (IWSSIP)*, 2009, pp. 1–4.

[7] N. Arulselvan, V. Ramachandran, and S. Kalyanasundaram, "Distributed power control mechanisms for HSDPA femtocells," in *Proc. IEEE Veh. Technol. conf. (VTC)*, 2009, pp. 1–5.

[8] X. Li, L. Qian, and D. Kataria, "Downlink power control in co-channel macrocell femtocell overlay," in *Proc. IEEE Int. Conf. on Information Science and System (CISS)*, 2009, pp. 383–388.

[9] Q. Su, A. Huango, Z. Wu, G. Yu, Z. Zhang, K. Xu, and J. Yang, "A distributed dynamic spectrum access and power allocation algorithm for femtocell networks," in *Proc. IEEE Int. Conf. on Wireless Commun. and Sig. Processing (WCSP)*, 2009, pp. 1–5.

[10] Y. Tokgoz, F. Meshkati, Y. Zhou, M. Yavuz, and S. Nanda, "Uplink interference management for HSPA+ and 1xEVDO femtocells," in *Proc. IEEE Global Telecom. Conf. (Globecom)*, 2003, pp. 1776–1780.

[11] M. Yavuz, F. Meshkati, and S. Nanda, "Interference management and performance analysis of UMTS/HSPA+ femtocells," *IEEE Commun. Mag.*, vol. 47, no. 9, pp. 102–109, Oct. 2009.

[12] J. Han-Shin, Y. Jong-Gwan, and M. Cheol, "A self-organized uplink power control for cross-tier interference management in femtocell networks," in *Proc. IEEE Military Commun. Conf. (MILCOM)*, 2009, pp. 1–6.

[13] V. Chandrasekhar, J. G. Andrews, T. Muharemovic, Z. Shen, and A. Gatherer, "Power control in two-tier femtocell networks," *IEEE Trans. on Wireless Commun.*, vol. 8, no. 8, pp. 4316–4328, 2009.

[14] H. Jo, C. Mun, J. Moon, and J. Yook, "Interference mitigation using uplink power control for two-tier femtocell networks," *IEEE Trans. on Wireless Commun.*, vol. 8, no. 10, pp. 4906–4910, 2009.

[15] V. Chandrasekhar and J. G. Andrews, "Uplink capacity and interference avoidance for two-tier femtocell networks," *IEEE Trans. on Wireless Commun.*, vol. 8, no. 7, pp. 3498–3509, 2009.

[16] L. Garcia, K. Pedersen, and P. Mogensen, "Autonomous component carrier selection: interference management in local area environments for lte-advanced," *IEEE Commun. Mag.*, vol. 47, no. 9, pp. 110–116, Oct. 2009.

[17] Y. Kim, S. Lee, and D. Hong, "Performance analysis of two-tier femtocell networks with outage constraints," *IEEE Trans. on Wireless Commun.*, vol. 9, no. 9, pp. 2695–2700, 2010.

[18] W. Yi, Z. Dongmei, and J. Hai, "A novel spectrum arrangement scheme for femto cell deployment in LTE macro cells," in *Proc. IEEE Int. Sym. on Personal, Indoor and Mobile Radio Commun. (PIMIC)*, 2010, pp. 6–11.

[19] "IEEE standard for local and metropolitan area networks part 16: Air interface for fixed broadband wireless access systems," *IEEE Std 802.16-2004 (Revision of IEEE Std 802.16-2001)*, pp. 1–857, 2004.

[20] G. RAN4, "Simulation assumptions and parameters for fdd henb rf requirements," *R4-092042*, May.

[21] L. H. H. Claussen and L. Samuel, "An overview of the femtocell concept," *Bell Labs Technical Journal*, vol. 13, no. 1, pp. 221–245, 2008.

[22] K. Yang, N. Prasad, and X. Wang, "An auction approach to resource allocation in uplink OFDMA systems," *IEEE Trans. on Signal Processing*, vol. 57, no. 11, pp. 4482–4496, Jun. 2009.

[23] H. Claussen, "Performance of macro- and co-channel femtocells in a hierarchical cell structure," in *Proc. IEEE Int. Sym. on Personal, Indoor and Mobile Radio Commun. (PIMIC)*, 2007, pp. 1–5.

[24] D. P. Bertsekas, "Auction algorithms," *Encycl. Optimiz.*

[25] "Femtocell designs sniff out cells: Enables self-organizing wireless networks," in *http://www.cellular-news.com/story/34526.php*.

[26] V. Erceg, L. Schumacher, and P. Kyritsi, "IEEE P802. 11 wireless LANs: TGn channel models," *IEEE 802.11 document 03/940r1*, 2003.

[27] ——, "WiMax evaluation methodology, version 2.1," in *http://www.wimaxforum.org/documents/documents/WiMAX System Evaluation Methodology V2.1*, 2008.

[28] C. So-In, R. Jain, and A. Tamimi, "Capacity evaluation for IEEE 802.16e mobile WiMAX," *Journal of Computer Systems, Networks, and Communications*, vol. 2010, no. Article ID 279807, pp. 12 pages, doi:10.1155/2010/279 807, 2010.

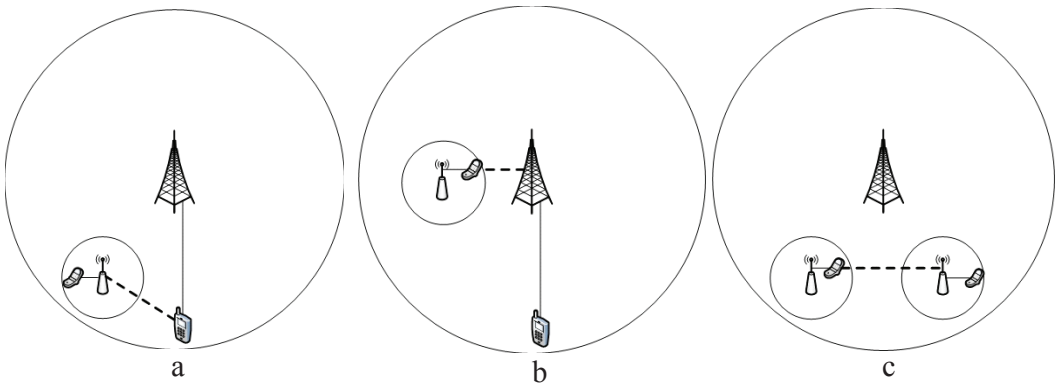

Fig. 1. (1) MU to FAP interference. (b) FU to MBS interference. (c) FU to FAP interference.

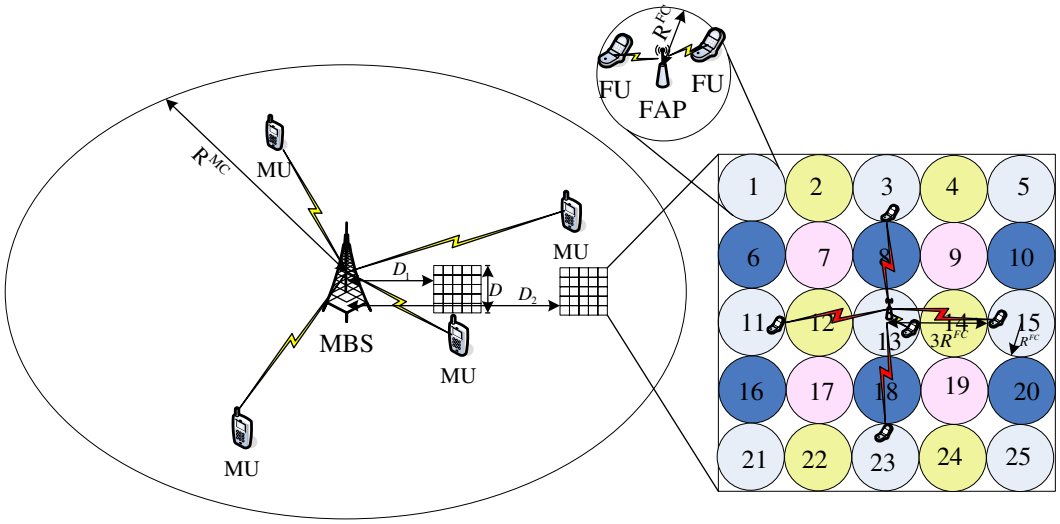

Fig. 2. A two-tier network of macrocell and femtocells.

TABLE I

SIMULATION PARAMETERS

Parameter	Value	Parameter	Value
femtocell radius R^{FC}	10m	FAP Ant. Gain G^F	0
Macrocell radius R^{MC}	500m	FAP Ant. Pattern	Omni
Carrier frequency (f_c)	2.5GHz	MU Minimum transmission power	10dBm
Bandwidth B	10MHz	MU Maximum transmission power	30dBm
Number of total subcarriers N	1024	FU mode transmission power	10dBm
Number of shared subcarriers N_f	256	AWGN power density (N_o)	-174dBm/Hz
MBS Ant. Gain G^M	15dB	MBS Ant. Patten	Omni
Number of active MUs M	128	Number of active FUs in each femtocell (L)	4
OFDMA symbol time T [28]	$102.8\mu s$	The weighting factor ω	1

TABLE II

VALUES OF $\text{SINR}_{\min}$ FOR DIFFERENT MODULATIONS [27].

QPSK	8.5dB
16-QAM	15dB
64-QAM	21dB

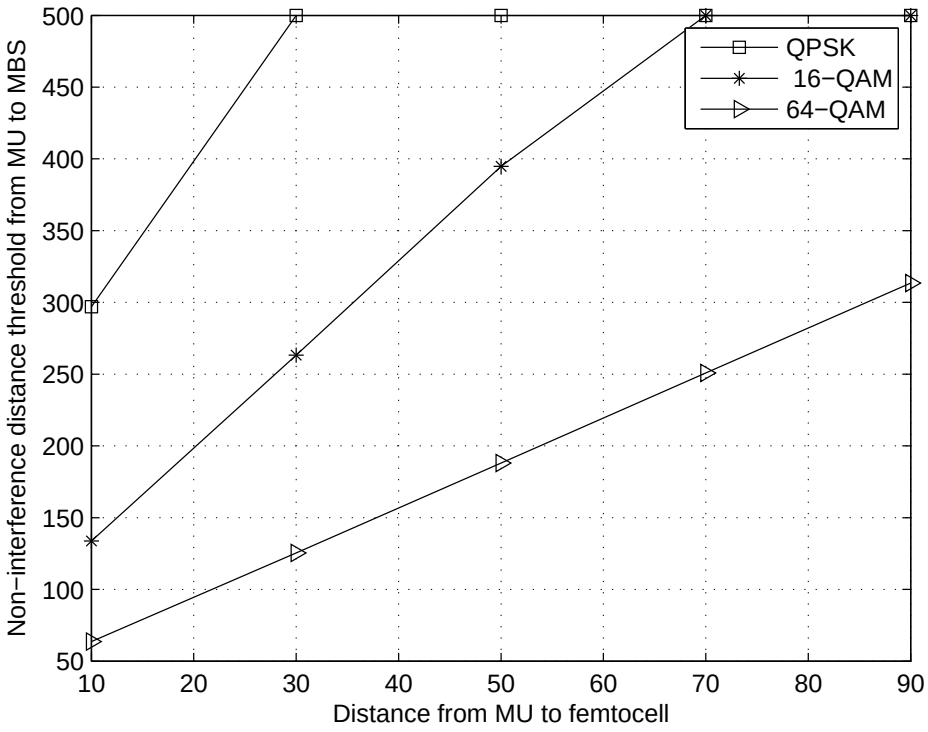

Fig. 3. $d_{\max}^{MU}$ as a function of d^{MF} for three modulation formats.

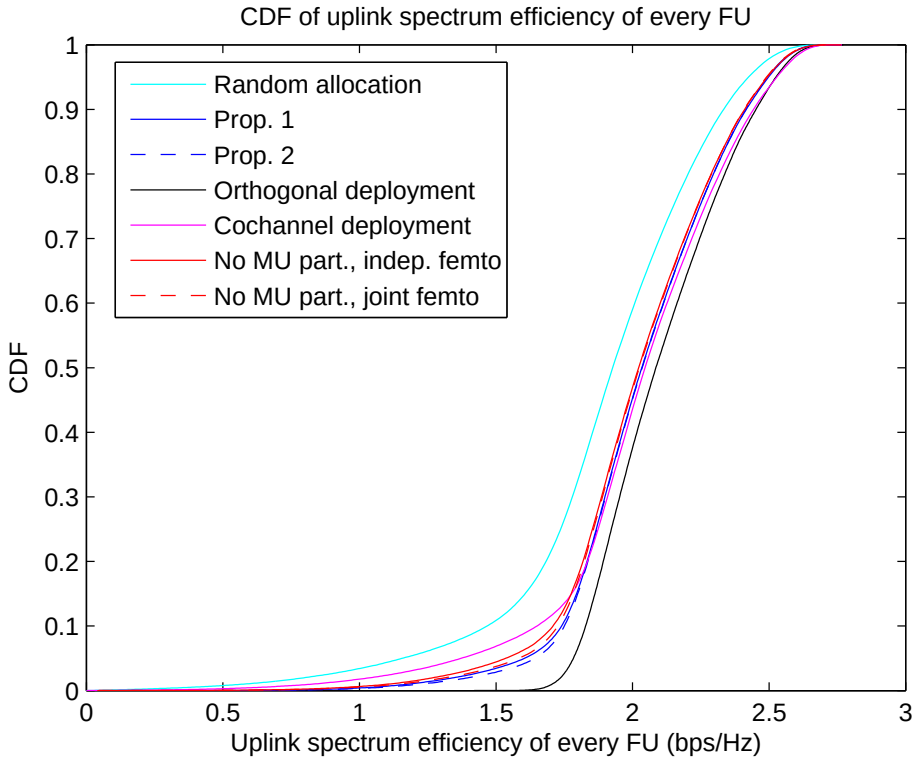

Fig. 4. CDF of uplink spectral efficiency of every FU.

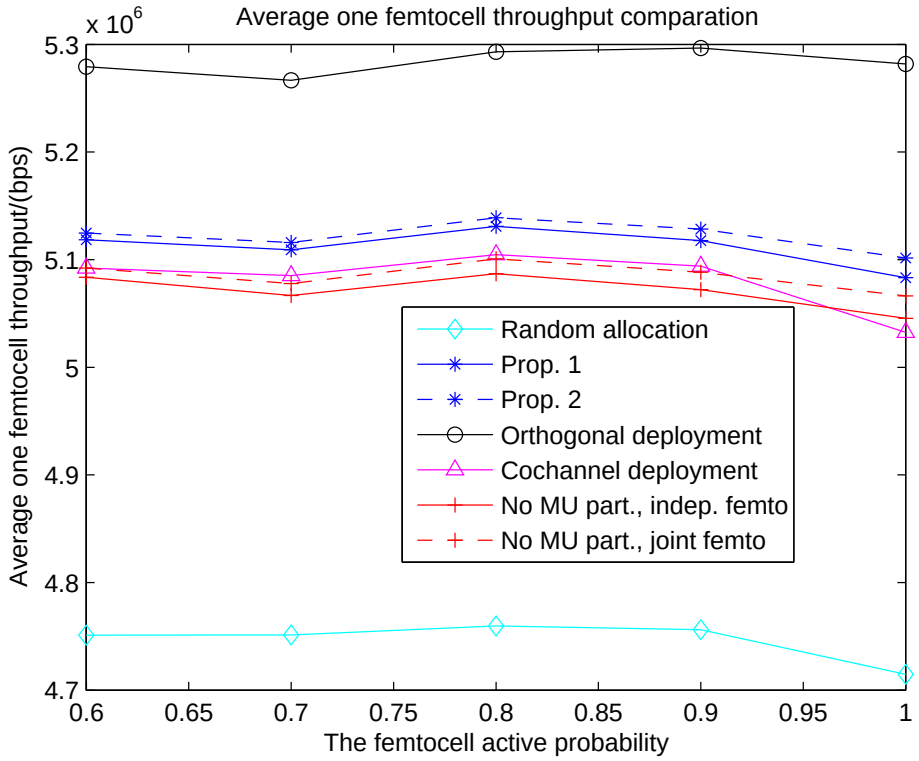

Fig. 5. Average one femtocell throughput versus active probability of FAP.

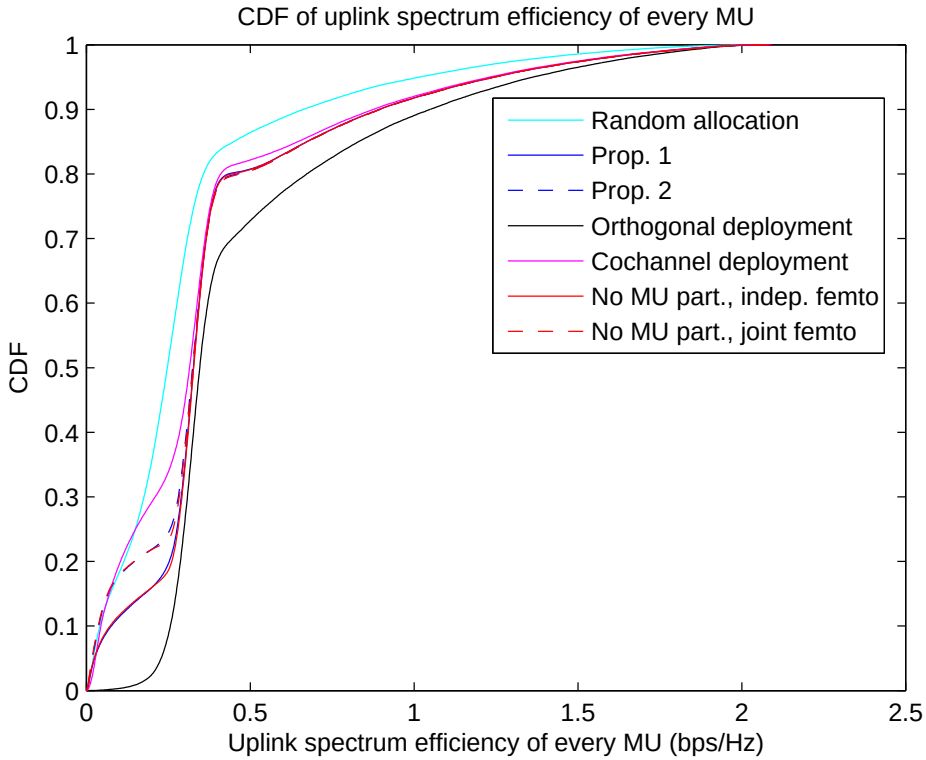

Fig. 6. CDF of uplink spectral efficiency of every MU.

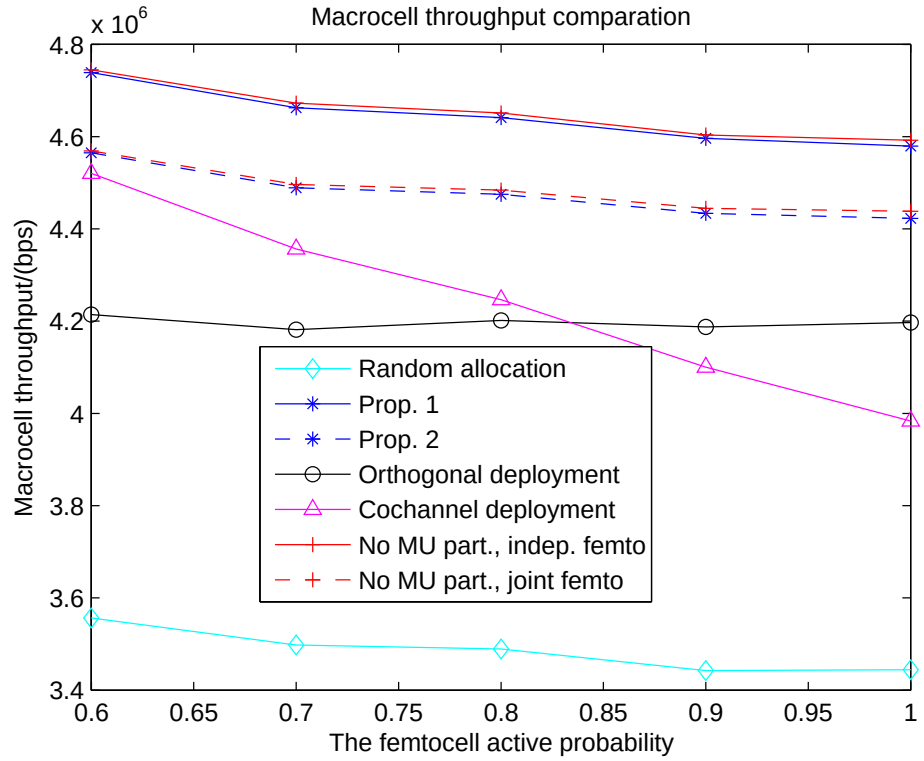

Fig. 7. Macrocell throughput versus active probability of FAP.

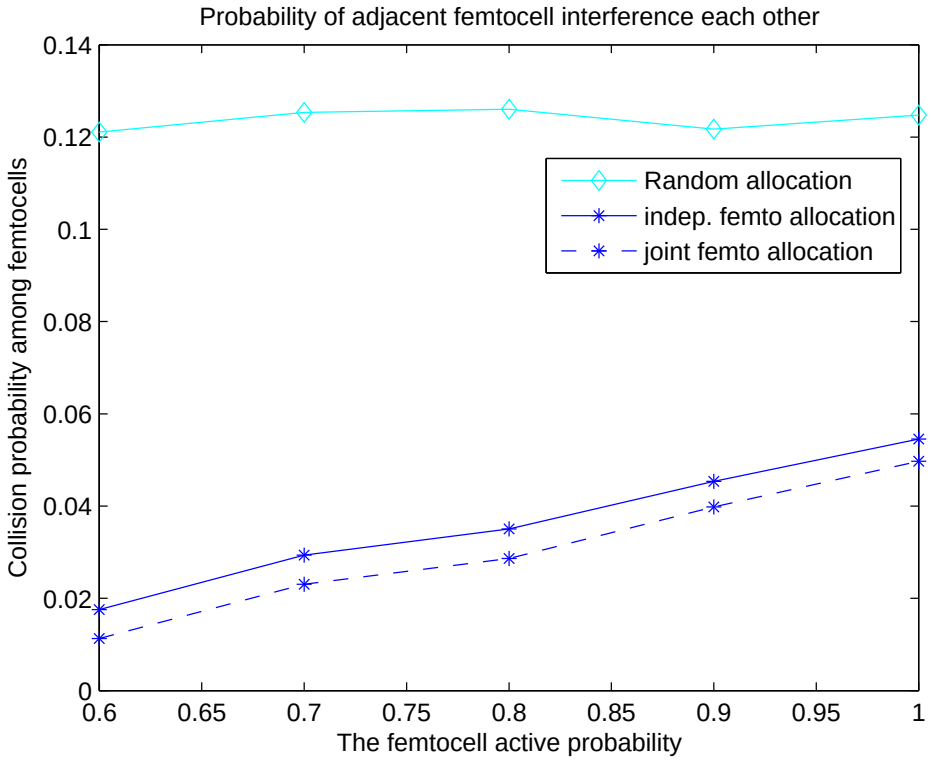

Fig. 8. Collision probability among femtocells versus active probability of FAP.

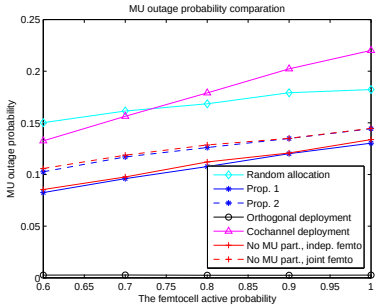

(a) MU outage probabilities versus active probability of FAP

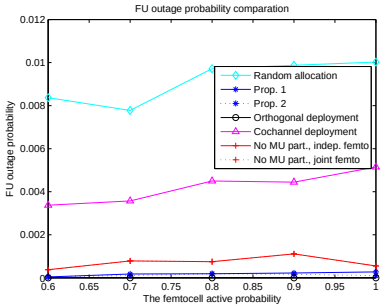

(b) FU outage probabilities versus active probability of FAP

Fig. 9. Outage probabilities of MU and FU

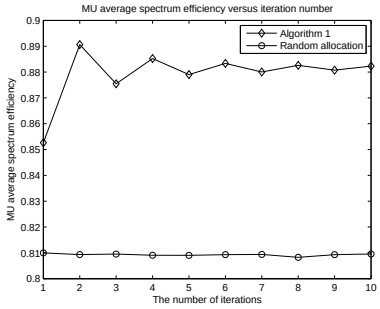

(a) MU average spectrum efficiency versus iteration number

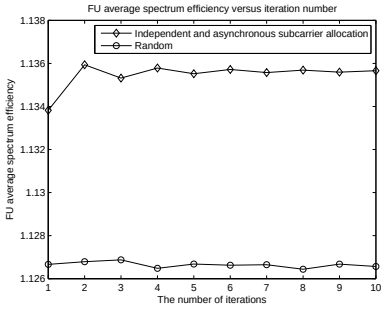

(b) FU average spectrum efficiency versus iteration number

Fig. 10. Convergence of proposed algorithms